

UNCLASSIFIED

Defense Technical Information Center  
Compilation Part Notice

ADP013120

TITLE: Spectroscopy of Inhomogeneous Strain in Silicon-Based Quantum Dots

DISTRIBUTION: Approved for public release, distribution unlimited  
Availability: Hard copy only.

This paper is part of the following report:

TITLE: Nanostructures: Physics and Technology International Symposium [8th] Held in St. Petersburg, Russia on June 19-23, 2000 Proceedings

To order the complete compilation report, use: ADA407315

The component part is provided here to allow users access to individually authored sections of proceedings, annals, symposia, etc. However, the component should be considered within the context of the overall compilation report and not as a stand-alone technical report.

The following component part numbers comprise the compilation report:

ADP013002 thru ADP013146

UNCLASSIFIED

## Spectroscopy of inhomogeneous strain in silicon-based quantum dots

A. Zaslavsky<sup>†</sup>, Jun Liu<sup>‡</sup>, B. R. Perkins<sup>†</sup> and L. B. Freund<sup>†</sup>

<sup>†</sup> Division of Engineering, Brown University, Providence, RI 02912, USA

<sup>‡</sup> Dept. of Physics, Brown University, Providence, RI 02912, USA

**Abstract.** Resonant tunneling is employed to probe the inhomogeneous strain in silicon-based quantum dots. When submicron structures are etched from a *p*-Si/SiGe/Si double-barrier heterostructure, the resonant  $I(V)$  peaks shift and develop a fine structure consistent with pronounced strain relaxation in the SiGe quantum well. We calculate the strain dependence on dot size by finite element techniques and convert the strain to an effective lateral confining potential. In sufficiently small dots, we find that the inhomogeneous strain confines carriers not only to the central core, as in GaAs-based dots, but also to a ring-like region at the perimeter. We probe the resulting density of states by magnetotunneling  $I(V, B)$  measurements.

### Introduction

When a semiconductor nanostructure, like a quantum wire or a quantum dot, is fabricated from strained epitaxially grown material, the originally homogeneous strain is replaced by geometry-specific strain gradients. The symmetry-based analytic treatment [1] for handling the biaxial strain in lattice-mismatched materials no longer suffices, particularly for quantum dots which lack translational symmetry altogether. Instead one turns to finite-element calculations of the strain field based on linear elastic models, but their applicability to structures whose size  $D$  might be down to tens of lattice constants is not self-evident. Thus, any experimental technique that is sensitive to inhomogeneous strains provides a valuable test bed for the validity of finite-element techniques for strained nanostructures — in our work, the experimental probe will be the resonant tunneling current-voltage  $I(V)$  measurements.

Further, inhomogeneous strain in semiconductor nanostructures is taking on additional technological relevance, as advances in strained layer epitaxy and ongoing device miniaturization promise the arrival of deep submicron bandgap-engineered devices, such as strained Si/SiGe HBTs for high-frequency analog and digital applications. Particularly interesting is the use of strain-driven self-assembly of quantum dots in semiconductor lasers [2] to enhance gain and shift the lasing wavelength. In such devices, strain relaxation is the key to the size and morphology of the quantum dots, as well as the optical transition energies.

Finally, it is important to note that inhomogeneous strains in quantum nanostructures can contribute to carrier localization in unpredictable ways. Over the past decade, quantum dots have been extensively investigated as systems containing a few spatially confined charge carriers [3–5]. However, most of these experiments probed dots made from lattice-matched GaAs/AlGaAs heterostructures, in which the carriers are confined to the central region of the dot by a roughly parabolic lateral potential arising from the gate potential or the pinning of the Fermi level at the surface. In our strained Si/SiGe quantum dots, the inhomogeneous-strain-induced lateral confinement potential is nonmonotonic, leading to an effective potential minimum near the perimeter of the dot. For sufficiently small dots,

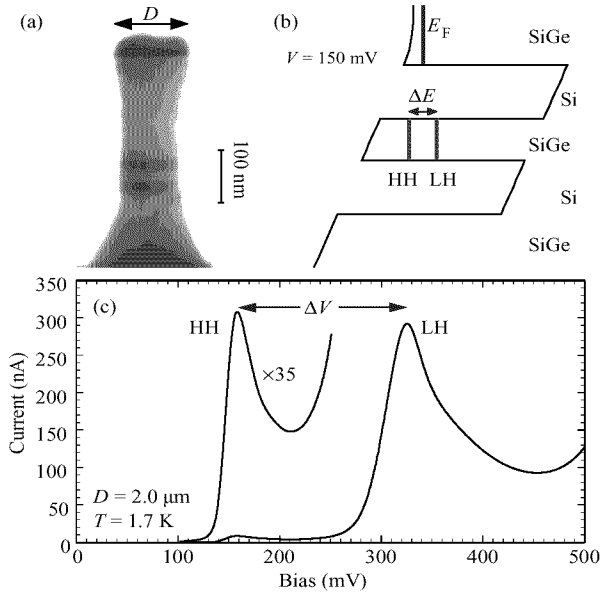


**Fig. 1.** (a) SEM micrograph of a representative double-barrier nanostructure with lateral dimension  $D \sim 0.15 \mu\text{m}$ . (b) Self-consistent potential profile of the Si/SiGe double-barrier active region at  $V = 150 \text{ mV}$ . (c) Resonant tunneling  $I(V)$  of a large  $D = 2 \mu\text{m}$  device at  $1.7 \text{ K}$ , with the HH peak magnified  $\times 35$  for clarity.

this potential confines the ground state to a one-dimensional (1D) ring-like region near the perimeter – a new type of structure expected to have interesting magnetic properties.

### 1. Tunneling and strain in SiGe double-barrier microstructures

Our devices begin with  $p\text{-Si/Si}_{1-x}\text{Ge}_x/\text{Si}$  double-barrier heterostructures described in detail in previous publications [6, 7, 8]. They are grown on  $p\text{-Si}$  substrates, with an undoped active region consisting of Si barriers confining a  $\text{Si}_{1-x}\text{Ge}_x$  QW that is  $35 \text{ \AA}$  wide with Ge content  $x = 0.25$  or  $0.2$  (corresponding to a lattice mismatch of  $\sim 1$  and  $\sim 0.8\%$  respectively). Outside the barriers are  $p\text{-Si}_{1-x}\text{Ge}_x$  emitter and collector regions that serve as reservoirs for tunneling holes.

When a bias  $V$  is applied between the emitter and collector, the holes in the emitter tunnel via the quantized 2D hole subbands, subject to the usual energy  $E$  and transverse momentum  $\mathbf{k}_\perp$  conservation rules [9]. In large devices, the strain in the SiGe well can be taken as biaxial and homogeneous, so the energies of the 2D subbands can be reliably calculated numerically [6]. Figure 1 shows an SEM photograph of a device, together with a self-consistent potential distribution in the active region under bias, and the  $I(V)$  characteristic of a large  $D = 2 \mu\text{m}$  Si/Si<sub>0.75</sub>Ge<sub>0.25</sub> device at  $T = 1.7 \text{ K}$ . The peaks correspond to tunneling through the two confined 2D subbands, labeled HH and LH for the heavy-hole and light-hole branches of the dispersion. The agreement with the predicted peak positions is excellent [6, 7], so the peak positions reflect the energies of the quantized states in the SiGe well. In particular, the energy separation  $\Delta E$  between the HH and LH subbands arises in part from the strain-induced splitting, which lifts the HH-LH degeneracy in the SiGe valence band [1, 10]. Thus, any significant change in the strain should be reflected in  $\Delta E$ .

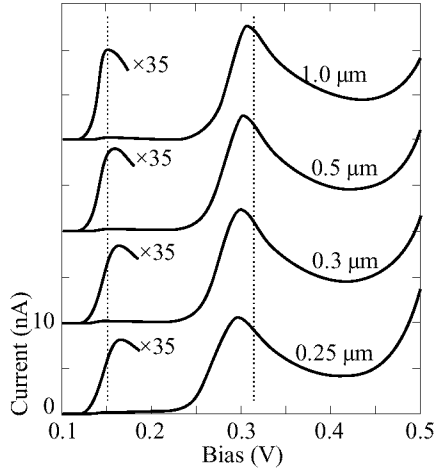


**Fig. 2.**  $I(V)$  characteristics with nominal lateral diameters of  $D = 1.0\text{--}0.25\ \mu\text{m}$  at 1.7 K. Current scale corresponds to the smallest device, other curves are rescaled and the HH peaks magnified for clarity. Vertical lines mark the HH and LH peak positions in large devices.

## 2. Average strain relaxation in SiGe double-barrier microstructures

When a narrow mesa is etched through the active region of our devices, the biaxially compressed SiGe strained layers can relax by lateral displacement at the sidewall. We first observed this effect experimentally some years ago [7] and it has been confirmed by others [11]. Figure 2 shows the effect in a series of identically fabricated Si/Si<sub>0.75</sub>Ge<sub>0.25</sub> devices with  $D$  ranging from 1 down to  $0.25\ \mu\text{m}$ . The  $I(V)$  curves exhibit a consistent shift of HH and LH peaks towards each other as  $D$  decreases, even as the  $I(V)$  lineshape remains largely unaffected. The effect is large, with changes in  $\Delta E$  indicating a significant amount of strain relaxation.

We compared the strain relaxation inferred from the data in Fig. 2 to finite-element simulations based on a linear elastic model, in which the cylindrical structure was allowed to relax to a minimum energy configuration [12]. The average values of strain relaxation predicted by these calculations agree quite well with our experimental data, with the dominant radial strain component  $\epsilon_{rr}$  relaxing to  $\sim 0.7$  of the full lattice-mismatch strain when  $D$  falls to  $0.3\ \mu\text{m}$ . Interestingly, the simulated strain relaxation in the SiGe layers is non-monotonic in the radial direction  $r_{\perp}$  and significant strain gradients exist throughout the SiGe well in sufficiently small structures,  $D \leq 0.25\ \mu\text{m}$ . The inhomogeneous strain leads to additional lateral quantization in the confined 2D subbands, which we first observed in [8].

## 3. Inhomogeneous strain in SiGe quantum dots

The calculated radial strain  $\epsilon_{rr}$  in the SiGe QW and the corresponding strain-induced lateral potential for HH states are shown in Fig. 3 as a function of  $r_{\perp}$  for  $D = 0.1\text{--}0.2\ \mu\text{m}$  devices with a Si<sub>0.8</sub>Ge<sub>0.2</sub> well. The inset shows the calculation geometry and lateral displacement of the strained SiGe layers. First consider the radial strain  $\epsilon_{rr}(r_{\perp})$  curves at the top of Fig. 3. For  $D = 0.2\ \mu\text{m}$ ,  $\epsilon_{rr}$  decreases gradually with  $r_{\perp}$  except for a region of increasing strain near the perimeter that extends  $\sim 100\ \text{\AA}$  and reaches  $\epsilon_{rr} \sim 0.6$ .

This strained ring-like region exists for all  $D$  [8], [12], but for devices much larger than

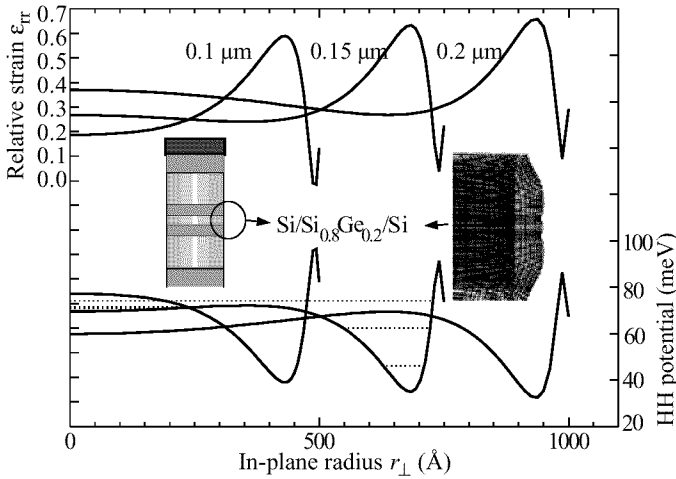


**Fig. 3.** The top curves show the calculated radial strain component  $\epsilon_{rr}(r_{\perp})$  for  $D = 0.1\text{--}0.2\ \mu\text{m}$  devices at the mid-plane of the  $\text{Si}_{0.8}\text{Ge}_{0.2}$  well (full strain is  $\epsilon_{rr} = 1$ ). Inset shows the magnified displacement of the finite-element mesh near the sidewall. The bottom curves are the corresponding in-plane confining potentials for the HH states as function of  $r_{\perp}$ . Dashed lines mark the confined ring subbands in a  $D \sim 0.15\ \mu\text{m}$  dot.

$D = 0.2\ \mu\text{m}$  it can be taken as a perturbation to the inner core. On the other hand, in small devices,  $D \leq 0.15\ \mu\text{m}$ , the ring at the perimeter becomes the most highly strained region in the device. The corresponding confining potential for HH states is shown by the bottom set of curves in Fig. 3: in the smallest dots, the strain would confine holes to a 1D ring at the perimeter.

Figure 4 shows the HH  $I(V)$  peak of a  $D \sim 0.15\ \mu\text{m}$  device fabricated from the  $\text{Si}/\text{Si}_{0.8}\text{Ge}_{0.2}$  double-barrier material, together with a reference lineshape from a large device. The  $I(V)$  lineshape exhibits very strong fine structure, corresponding to strong lateral quantization due to inhomogeneous strain [3]. A full-blown calculation of the expected density of states in such a quantum dot in the presence of the inhomogeneous strain is complicated by the anisotropy and nonparabolicity of the in-plane effective mass in the quantum well, but taking the in-plane HH effective mass  $m^* \sim 0.25$  we obtain several radially quantized subbands in the perimeter ring separated by a few meV, see Fig. 3. Since quantized ring-like subbands overlap in energy with the states in the relaxed central core, they would be expected to contribute structure on top of the relatively smooth overall HH peak lineshape. The energy separation of the ring subbands extracted from the structure in the  $I(V)$  agrees reasonably with the calculations of Fig. 3.

#### 4. Magnetotunneling spectroscopy of strained SiGe quantum dots

The additional ring-like confinement of hole states in sufficiently small inhomogeneously strained SiGe quantum dots provides a new and interesting system for magnetic field effects. Figure 5(a) shows the evolution of the HH  $I(V)$  peak fine structure in magnetic fields  $B = 0\text{--}10\ \text{T}$  ( $B \parallel I$ ), while Fig. 5(b) indicates the evolution of the  $I(V)$  peaks converted to an energy scale. In the absence of inhomogeneous strain, the  $B$  field would compress the 2D subband density of states into Landau levels. Given a constant in-plane effective mass, as in  $n\text{-GaAs}/\text{AlGaAs}$  double-barrier structures, the Landau level separation would

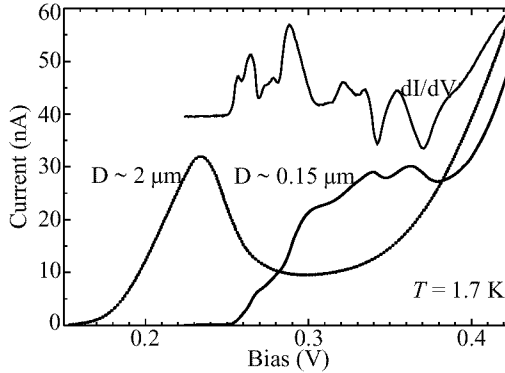


**Fig. 4.** HH resonant peak  $I(V)$  and  $dI/dV$  characteristics of a  $D \sim 0.15 \mu\text{m}$  Si/Si<sub>0.8</sub>Ge<sub>0.2</sub> dot. The dashed line shows the smooth HH  $I(V)$  lineshape in a large device.

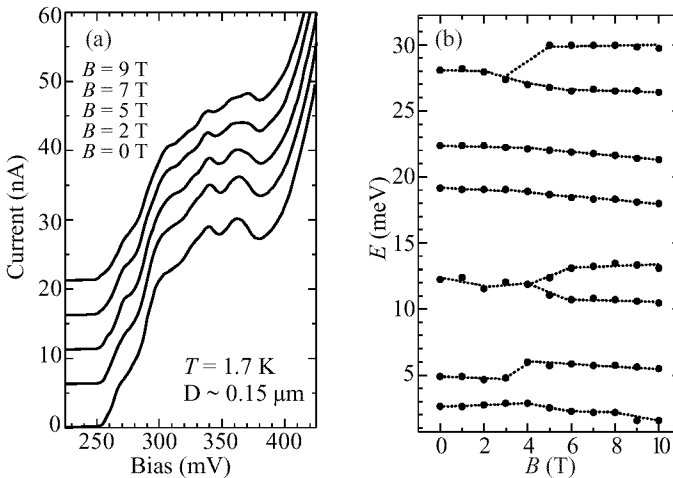


**Fig. 5.** (a) Evolution of HH  $I(V, B)$  lineshape of the  $D \sim 0.15 \mu\text{m}$  dot with  $B$ ; (b)  $B$ -field-induced shifts and splittings in the density of states peaks in the dot.

be linear in  $B$  and the  $I(V, B)$  lineshape would show equally spaced features falling on the usual Landau fan diagram [13]. Given the complex, nonparabolic dispersion of holes in SiGe quantum wells, the Landau level spectrum is quite complicated even in a uniformly strained well [14] and  $B$ -induced structure has only been seen experimentally at fairly large  $B$  [6]. The data in Fig. 5 shows rather complex behavior, with some of the peaks shifting towards lower energy with  $B$ , others appearing to repel each other, and some even splitting around  $B \sim 5$  T. A theoretical analysis of ring-like hole states in a  $B$  field remains to be performed.

## 5. Conclusions

We have investigated the effects of size-induced strain relaxation in strained SiGe quantum dots. Our data indicate that large strain relaxation and nonmonotonic strain gradients appear in deep submicron structures, in agreement with finite element simulations. We also see evidence for confinement of carriers to ring-like regions at the perimeter due to inhomogeneous strain.

geneous strain. Our measurements prove resonant tunneling to be a viable spectroscopic probe for strain effects in individual nanostructures.

#### *Acknowledgements*

The work at Brown has been supported by an NSF Career award for A. Z. (DMR-9702725), ONR (N00014-95-1-0239), the Sloan Foundation, and the MRSEC Program of the NSF (DMR-9632524).

#### **References**

- [1] G. L. Bir and G. E. Pikus, *Symmetry and Strain-Induced Effects in Semiconductors*, New York, Wiley, 1974.
- [2] D. Bimberg, M. Grundmann and N. N. Ledentsov, *Quantum Dot Heterostructures*, New York, Wiley, 1999.
- [3] Bo Su, V. J. Goldman and J. E. Cunningham, *Science* **255**, 313 (1992).
- [4] T. Schmidt, M. Tewordt, R. H. Blick *et al.*, *Phys. Rev. B* **51**, 5570 (1995).
- [5] S. Tarucha, D. G. Austing, T. Honda *et al.*, *Phys. Rev. Lett.* **77**, 3613 (1996).
- [6] A. Zaslavsky, D. A. Grützmacher, S. Lin *et al.*, *Phys. Rev. B* **47**, 16036 (1993).
- [7] A. Zaslavsky, K. R. Milkove, Y. H. Lee *et al.*, *Appl. Phys. Lett.* **67**, 3921 (1995).
- [8] C. D. Akyüz, A. Zaslavsky, L. Freund *et al.*, *Appl. Phys. Lett.* **72**, 1739 (1998).
- [9] S. Luryi, *Appl. Phys. Lett.* **47**, 490 (1985).
- [10] For a concise treatment of SiGe, see R. People, *Phys. Phys. B* **32**, 1405 (1985).
- [11] P. W. Lukey, J. Caro, T. Zijlstra, *et al.*, *Phys. Rev. B* **57**, 7132 (1998).
- [12] H. T. Johnson, L. B. Freund *et al.*, *J. Appl. Phys.* **84**, 3714 (1998).
- [13] See, for example, V. J. Goldman, D. C. Tsui and J. E. Cunningham, *Phys. Rev. B* **35**, 9387 (1987) and references therein.
- [14] S.-R. Eric Yang, D. A. Broido and L. J. Sham, *Phys. Rev. B* **32**, 6630 (1985).